



RESEARCH PAPER

The *Arabidopsis thaliana* elongator complex subunit 2 epigenetically affects root development

Yuebin Jia¹, Huiyu Tian¹, Hongjiang Li², Qianqian Yu¹, Lei Wang³, Jiri Friml² and Zhaojun Ding^{1*}

¹ The Key Laboratory of Plant Cell Engineering and Germplasm Innovation, Ministry of Education, College of Life Science, Shandong University, Jinan 250100, China

² Institute of Science and Technology Austria, 3400 Klosterneuburg, Austria

³ Key Laboratory of Plant Molecular Physiology, Institute of Botany, Chinese Academy of Sciences, Beijing 100093, China

* To whom correspondence should be addressed. E-mail: dingzhaojun@sdu.edu.cn

Received 16 February 2015; Revised 8 April 2015; Accepted 15 April 2015

Editor: James Murray

Abstract

The elongator complex subunit 2 (ELP2) protein, one subunit of an evolutionarily conserved histone acetyltransferase complex, has been shown to participate in leaf patterning, plant immune and abiotic stress responses in *Arabidopsis thaliana*. Here, its role in root development was explored. Compared to the wild type, the *elp2* mutant exhibited an accelerated differentiation of its root stem cells and cell division was more active in its quiescent centre (QC). The key transcription factors responsible for maintaining root stem cell and QC identity, such as AP2 transcription factors *PLT1* (*PLETHORA1*) and *PLT2* (*PLETHORA2*), GRAS transcription factors such as *SCR* (*SCARECROW*) and *SHR* (*SHORT ROOT*) and WUSCHEL-RELATED HOMEBOX5 transcription factor *WOX5*, were all strongly down-regulated in the mutant. On the other hand, expression of the G2/M transition activator *CYCB1* was substantially induced in *elp2*. The auxin efflux transporters *PIN1* and *PIN2* showed decreased protein levels and *PIN1* also displayed mild polarity alterations in *elp2*, which resulted in a reduced auxin content in the root tip. Either the acetylation or methylation level of each of these genes differed between the mutant and the wild type, suggesting that the ELP2 regulation of root development involves the epigenetic modification of a range of transcription factors and other developmental regulators.

Key words: Auxin ELP2, epigenetics, root.

Introduction

The maintenance of a functional root system makes an important contribution to a plant's capacity to adapt to instability in its growing environment. At the root apical meristem, root stem cells deliver the cells that differentiate to form the various tissue types found in the root (Dolan *et al.*, 1993). Stem cell identity within the root meristem is maintained by signals generated from cells in the quiescent centre (QC) (Vernoux and Benfey, 2005). The mitotically less active QC, together with its surrounding stem cells, constitutes the 'root stem cell niche', a structure that is essential for the maintenance of root growth (Sabatini *et al.*, 2003). The specification

of cell identity within the root stem cell niche is determined by the activity of a number of transcription factors: these include members of both the AP2 (*PLTs*) and GRAS (*SCR* and *SHR*) transcription factor families (Helariutta *et al.*, 2000; Sabatini *et al.*, 2003; Aida *et al.*, 2004; Galinha *et al.*, 2007). *PLT* proteins are not only involved in QC specification during embryogenesis but also have a more general role in the maintenance of root stem cell niche identity. In loss-of-function mutants, the embryonic root does not form, while the expression of *PLT* in the shoot is sufficient to specify root identity in shoot (Aida *et al.*, 2004; Galinha *et al.*, 2007). Both

SHR and SCR affect radial patterning in the root, and are also required for QC specification and root stem cell niche maintenance (Helariutta *et al.*, 2000; Sabatini *et al.*, 2003). The homeodomain transcription factor *WOX5* is specifically expressed in the QC in the wild-type (WT) plant. Its loss-of-function results in the formation of enlarged QC cells and promoted differentiation of the distal stem cells, but has no observable effect on either root growth or the size of the more proximal meristem cells; its over-expression blocks the differentiation of distal stem cells, thereby inducing the formation of multiple layers of distal stem cells. The primary function of *WOX5* appears to be to maintain distal stem cell identity (Sarkar *et al.*, 2007).

Root stem cell niche identity is also regulated by auxin and cytokinin (Dello Ioio *et al.*, 2007; Ding and Friml, 2010). Auxin initiates, organizes and maintains the root stem cell niche (Benjamins and Scheres, 2008), while the effect of cytokinin is to modulate the auxin pathway or polar auxin transport (Dello Ioio *et al.*, 2008; Ruzicka *et al.*, 2009). Auxin and cytokinin act antagonistically to define root apical meristem size by promoting, respectively, cell division and differentiation (Dello Ioio *et al.*, 2007). The maintenance of the root stem cell niche depends on the establishment of an auxin concentration gradient, which peaks at the stem cell niche. The stability of this gradient relies on both PIN-mediated distribution and its local synthesis (Blilou *et al.*, 2005; Grieneisen *et al.*, 2007; Tian *et al.*, 2013, 2014).

The eukaryotic elongator complex consists of an ELP1, ELP2 and ELP3 core and an accessory ELP4, ELP5 and ELP6 subcomplex (Wittschieben *et al.*, 1999; Kim *et al.*, 2002; Nelissen *et al.*, 2010; Versees *et al.*, 2010). It participates in acetylation, methylation/demethylation, exocytosis and tRNA modification (Kim *et al.*, 2002; Creppe *et al.*, 2009; Chen *et al.*, 2011; Defraia *et al.*, 2013; Wang *et al.*, 2013). In *Arabidopsis thaliana*, it mediates part of the response to biotic and abiotic stress, as well as being involved in the determination of leaf patterning (Nelissen *et al.*, 2005, 2010; Zhou *et al.*, 2009; Xu *et al.*, 2011; Defraia *et al.*, 2013). Previous studies also showed that the *elp1*, *elp3*, *elp4* mutants have defected root growth, however, the detailed mechanism was not well studied (Nelissen *et al.*, 2005). Here, we mapped *elp2* mutant according to its root stem cell defective phenotype and thoroughly investigated the role of *ELP2* on root development.

Materials and methods

Plant materials and growth conditions

The transgenic *A. thaliana* lines used were *WOX5:GFP* (Sarkar *et al.*, 2007); *CYCB1;1:GUS* (Colon-Carmona *et al.*, 1999); *DR5:GUS* (Ulmasov *et al.*, 1997); *DR5rev:GFP* (Benkova *et al.*, 2003); *PIN1:PIN1-GFP* (Benkova *et al.*, 2003); *PIN2:PIN2-GFP* (Blilou *et al.*, 2005); *PLT1 pro:CFP*, *PLT1 pro:PLT1-YFP*, *PLT2 pro:CFP*, and *PLT2 pro:PLT2-YFP* (Kornet and Scheres, 2009); *QC25* (Sabatini *et al.*, 2003); *SCRpro:SCR-GFP* (Di Laurenzio *et al.*, 1996); *SHRpro:SHR-GFP* (Nakajima *et al.*, 2001). The mutant *elp2*, and *elp6* are from an ethyl methanesulfonate mutagenized populations, *elp1* (*SALK_004690*) and *elp4* (*SALK_079193*) are from the *Arabidopsis* Stock Center, which are all in the Columbia (Col-0) background (Nelissen *et al.*, 2005; Zhou *et al.*, 2009). Seeds were

surface-sterilized by exposure to chlorine gas, sown on solidified Murashige and Skoog (1962) medium (MS medium), held for 2 d at 4°C, then raised under a 16 h photoperiod at 19°C for a further 5 d.

TAIL-PCR

DNA was extracted from leaves of WT ecotype Col-0 and the *elp2* mutant using a CTAB-based method. The primary PCR was primed with the T-DNA specific *Lba1* and a degenerate *AD* primer (sequences given in Supplementary Table S1). The secondary PCR was based on *Lbb1.3* and an *AD* primer, using a diluted aliquot of the primary PCR as the template. The tertiary PCR was based on *Lbb1* and an *AD* primer, using a diluted aliquot of the secondary PCR as the template. The amplicons were separated by agarose gel electrophoresis and the *dsr1* specific band compared to the WT (Col) was sequenced to find the T-DNA boundary sequence.

GUS, EdU and lugol staining

Staining of seedling roots for β -glucuronidase (GUS) activity was carried out by incubation at 37°C in 0.05M NaPO₄ buffer (pH 7.0), 5mM K₃Fe(CN)₆, 5mM K₄Fe(CN)₆ and 2mM X-glucuronide. Once the colour had developed, the material was passed through an ethanol series (70%, 50% and 20%) before mounting in 70% chloral hydrate plus 10% glycerol. EdU staining was performed following the protocol supplied with the Click-iT® EdU Alexa Fluor® 555 Imaging kit (Invitrogen). Detection of starch granules in the root tip followed staining in Lugol's solution for 1–2 min, after which the material was mounted in chloral hydrate as above.

RNA analysis

Seedlings were grown on MS medium for 5 d, after which the distal 2 mm of the roots were harvested for RNA extraction. Total RNA was isolated using a RNeasy® Mini Kit (Qiagen) and the first strand of cDNA was synthesized from a 2 μ g aliquot using a Transcriptor First Strand cDNA Synthesis kit (Roche) following the manufacturer's protocol. Quantitative real-time PCRs (qRT-PCRs) were based on the CFX Connect™ Real-Time System (Bio-Rad) and FastStart Universal SYBR Green Master mix (Roche). Three biological replicates were included, each of which was represented by three technical replicates. *AtACTIN2* was used as the reference sequence.

Chromatin immunoprecipitation (ChIP) assay

ChIP was used to quantify the acetylation level of the set of selected genes. The assay was based on an ~3g sample of two-week-old seedlings, following the Wang *et al.*, (2013) protocol. After *in vivo* cross-linking and tissue lysis, DNA was sheared by sonication and evaluated by agarose gel electrophoresis. The extracted nucleosomes were precleared using 40 μ l protein A agarose beads (Invitrogen), after which was added 2–3 μ g Ac-Histone H3 (Lys-9/14) antibody (sc-8655-R; Santa Cruz Biotechnology) before incubation at 4°C overnight. After de-cross-linking, DNA was extracted and precipitated using triple volumes of ethanol, NaAc, and glycogen. The resulting DNA was used as the template for a qRT-PCR, based on primers detailed in Supplementary Table S1. The acetylation level in each sample was normalized to both input DNA and *AtACTIN2* as described elsewhere (Mosher *et al.*, 2006). The Chromatin immunoprecipitation (ChIP) assay was done three times independently. The data represent mean values with their associated SD (n=3), *P* < 0.05.

Bisulfite sequencing

Genomic DNA was extracted with a CTAB protocol from ~1 g seedlings harvested from plants raised for two weeks on MS medium. About 2 μ g DNA was treated with an EpiTect® Bisulfite kit (Qiagen). Strand-specific and bisulfite-specific primers (see Supplementary Table S1) were designed using MethPrimer software (<http://www>

urogene.org/methprimer/). The amplicons were introduced into a pEASY-T1 simple vector (Tiangen) for sequencing, and the resulting sequences were analysed using DNAMAN software. Each sample was represented by three biological replicates.

Immunolocalization assay

PIN1 and PIN2 were immunolocalized as described elsewhere (Dai *et al.*, 2012).

Phenotypic analysis, microscopy, statistics

Seedlings grown on MS were scanned using EPSON PERFECTION V700 PHOTO, and root length was measured by Image J. Root meristems were analysed on seedlings mounted in HCG solution (Chloral hydrate:water:glycerol=8:3:1). Root meristem size was assessed as the cell number from the QC to the first elongating cell in the cortex cell file. Root micrographs were photographed using OLYMPUS BX53. Confocal imaging was obtained using an LSM-700 laser-scanning confocal microscope (Zeiss). Five-day-old seedling root tips were stained in propidium iodide.

Data presented are mean values of at least three biological repeats with SD. The statistical significance was analysed by Student's t-test analysis.

Results

The elp2 mutant shows defective root stem cell niche maintenance

A search for T-DNA mutants displaying a defective root stem cell niche maintenance phenotype identified *drs1*, a mutant that exhibited enhanced root distal stem cell differentiation and increased mitotic activity in its QC (Fig. 1). When five-day-old seedlings were exposed for 24 h to EdU [a thymidine

analogue used to mark S-phase progression (Vanstraelen *et al.*, 2009)], a stronger level of fluorescence was observed in the nuclei of mitotically active cells in the mutant than in WT, due to the coupling of EdU with Aexa Fluor 555. This assay indicated that mitotic activity was enhanced in *elp2* QC cells (Fig. 1E, F). The QC specific transcription factor *WOX5* was also strongly down-regulated (Fig. 1C, D), as was the signal produced by the QC marker *QC25* (Fig. 1G, H).

A TAIL-PCR analysis identified that in the mutant, the *ELP2* locus (At1g49540) had been interrupted by the insertion of a T-DNA element within the second intron (Supplementary Figs S1, S2). The hybrid between *drs1* and *elp2* [the latter differs from WT by a G to A transition at the acceptor splice site of the fifth intron (Zhou *et al.*, 2009)], just like the parental mutant lines, displayed both enhanced root distal stem cell differentiation and increased QC division, confirming that the defective root phenotype expressed by *drs1* was caused by a lesion in *ELP2*. We renamed the *elp2* mutant from EMS populations (Zhou *et al.*, 2009) as the *elp2-6*, and renamed the *drs1* as the *elp2-7* following the *elp2-2*, *elp2-3*, *elp2-4*, *elp2-5* identified previously (Nelissen *et al.*, 2005; DeFraia *et al.*, 2010). The *elp2-7* was used for most of the analysis and termed *elp2* afterwards in this paper. Mutations affecting other subunits of the elongation complex exhibited similar defective root stem cell niche maintenance (Supplementary Fig. S3).

The elp2 mutant's root meristem is reduced in size

In addition to the root stem cell niche identity defect, the *elp2* mutant also produced shorter roots than the WT seedlings

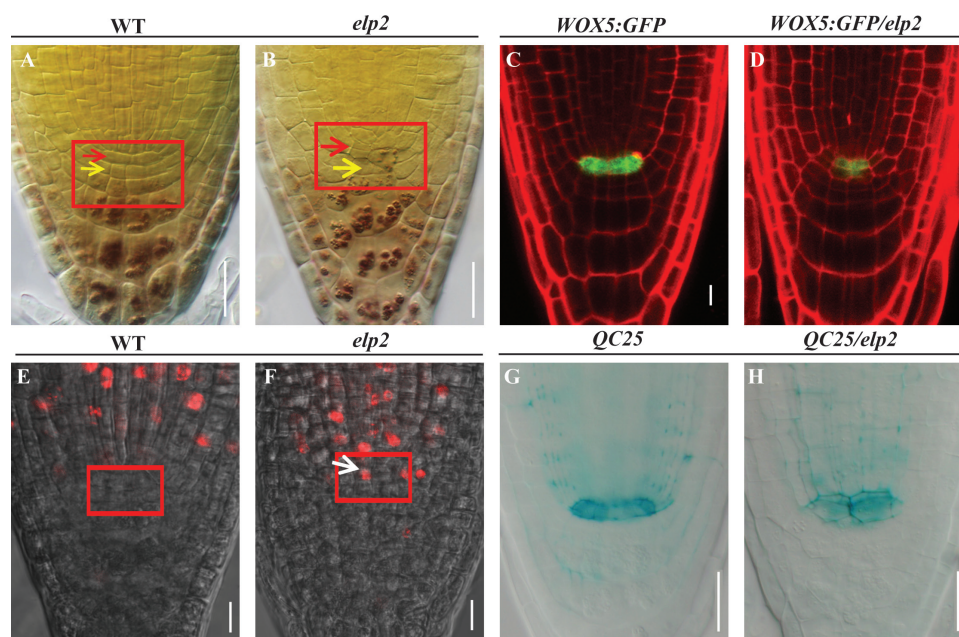


Fig. 1. The *elp2* mutant is defective with respect to root stem cell niche maintenance. Lugol stained (A) WT and (B) *elp2* roots. Cell division in the mutant QC is enhanced (red arrowheads), while its distal stem cells are deficient in starch (yellow arrowheads). The root stem cell niche is shown boxed. Confocal micrographs of (C) WT and (D) *elp2* plants expressing the transgene *WOX5:GFP*; the level of expression in the mutant is lower than in WT. Confocal micrographs illustrating the incorporation of EdU into (E) WT and (F) *elp2* QC cells. The fluorescent signals show that the mutant QC is in a state of active division (white arrowheads). The QC is shown boxed. *QC25* is expressed at a higher level in (G) the WT than in (H) the *elp2* mutant. Bars: 20 μ m (A, B, G, H); 10 μ m (C–F). (This figure is available in colour at JXB online.)

(Fig. 2A, B, Supplementary Fig. S4). This shortening was a result of smaller elongation (EZ) and meristem (MZ) zones (Fig. 2D, E). Cell number in the MZ and cell length in the EZ were both reduced compared to the WT (Fig. 2C, F), suggesting that *ELP2* affects both cell proliferation and cell elongation.

The down-regulation of transcription factors in the *elp2* mutant

To determine whether the effects of *ELP2* on root stem cell niche maintenance is dependent on the well characterized root stem cell niche-defining transcription factors, we examined the expression of AP2 transcription factors such as *PLT1* and *PLT2* and GRAS transcription factors such as *SCR* and *SHR* (Helariutta et al., 2000; Sabatini et al., 2003; Aida et al., 2004; Galinha et al., 2007) in *elp2*. The expression of both *PLT1 pro:PLT1-YFP* (Fig. 3C, D) and *PLT2 pro:PLT2-YFP* (Fig. 3G, H) was strongly reduced in *elp2* compared to the levels achieved in the WT, and the *PLT1 pro:CFP* and *PLT2 pro:CFP* behaved similarly (Fig. 3A, B, E, F). Consistently, a qRT-PCR assay showed that the expression level of *PLT1* and *PLT2* was lower in the *elp2* mutant than in the WT (Fig. 3I, J). Thus the evidence was that *ELP2* affected the transcription of both *PLT1* and *PLT2*. The expression of

SHR and *SCR* was investigated by comparing the expression of both *SCR pro:SCR-GFP* and *SHR pro:SHR-GFP* in both *elp2* and WT. Both transgenes were strongly down-regulated in the mutant (Fig. 4A–D), a result that was confirmed by a qRT-PCR assay (Fig. 4E, F).

ELP2 is required for cell-cycle progression in the root

The increased QC division and reduced root meristem cell numbers in *elp2* suggest that *ELP2* is required for proper cell-cycle progression in the root. Cells at the G2-M phase were visualized by the transgene *CYCB1;1:GUS* which reflects the cell cycle activity, however timely degradation of proteins is necessary to ensure the access of M phase (Colon-Carmona et al., 1999). In tobacco, the nondegradable Cyclin B1 results in abnormal cytokinesis and endomitosis (Weingartner et al., 2004). We observed that accumulation of the *CYCB1;1:GUS* signal in root meristem of *elp2* was much stronger than that in the WT (Fig. 5A, B). In addition, stronger staining in the root QC of *elp2* is consistent with the enhanced cell division in QC (Fig. 5A, B). Next, using qRT-PCR assays, we compared the *CYCB1;1* expression level in the *elp2* mutation and WT. In line with GUS staining, the *elp2* mutant has high *CYCB1;1* expression in the root (Fig. 5C). Therefore, our results showed that *ELP2* is required for cell-cycle progression in the root.

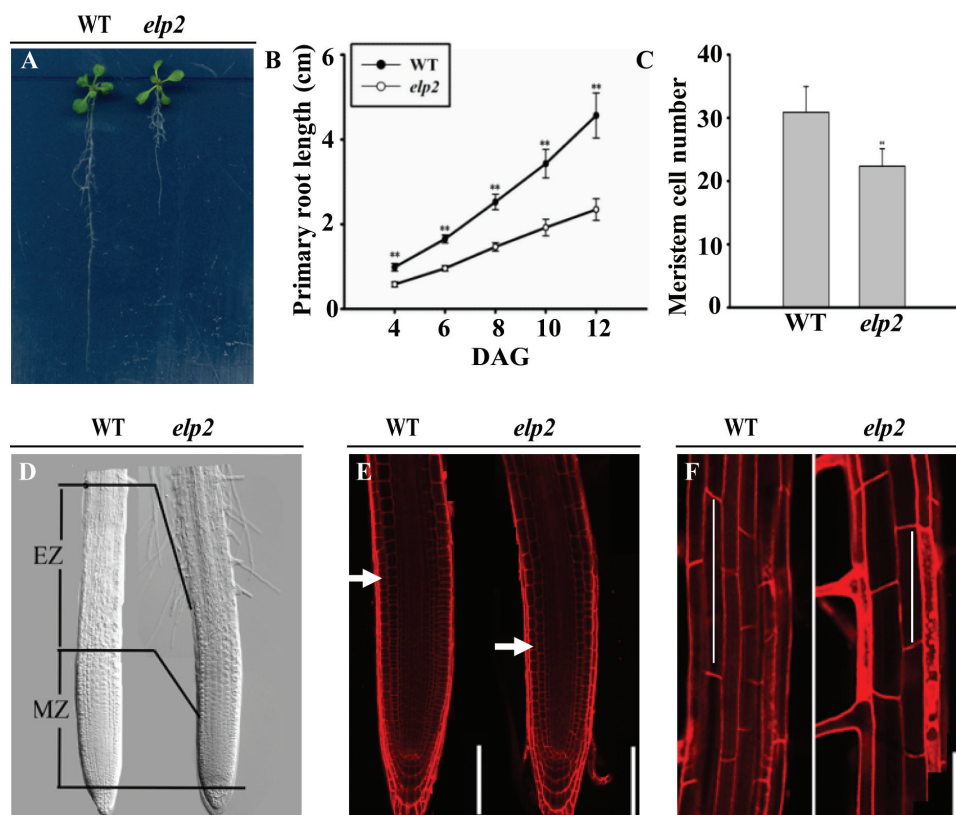


Fig. 2. The foreshortening of the roots produced by the *elp2* mutant reflects a reduced level of cell proliferation and cell elongation. (A) Roots of 12-day-old seedlings of WT and *elp2*. (B) Primary root growth of WT and *elp2* seedlings 4 d post germination. The data represent the mean and SD ($n=40$) derived from at least three independent experiments. (C) Variation in root meristem cell number of five-day-old WT and *elp2* seedlings. Cell numbers counted from the QC to the TZ. The data represent the mean and SD ($n=20$) derived from at least three independent experiments. (D) Representative five-day-old WT and *elp2* seedlings illustrating that the latter develop a reduced MZ and EZ. (E) Five-day-old WT and *elp2* seedlings. The cortex TZ is indicated by white arrowheads. (F) Epidermal cell length of the DZ in six-day-old WT and *elp2* seedlings. Bars, 50 μ m (E, F). **, $P<0.001$ (This figure is available in colour at JXB online.)

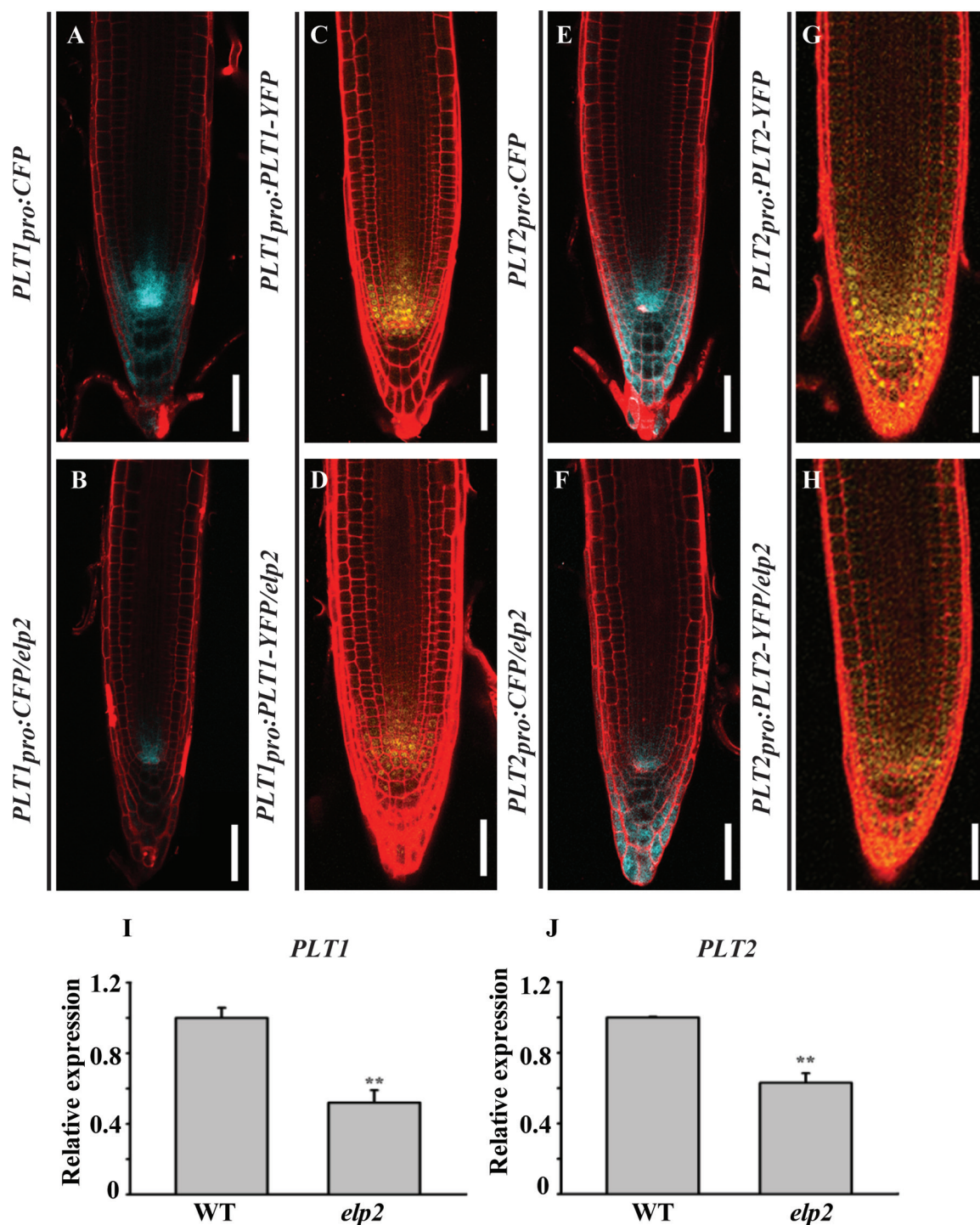


Fig. 3. *PLT1* and *PLT2* expression is reduced in the *elp2* mutant. Expression of the transgenes (A, B) *PLT1**pro*:CFP, (C, D) *PLT1**pro*:*PLT1*-YFP, (E, F) *PLT2* *pro*:CFP, (G, H) *PLT2* *pro*:*PLT2*-YFP. qRT-PCR assay of the transcription of (I) *PLT1* and (J) *PLT2*. The data represent mean values with their associated SD ($n=3$); **, $P<0.001$. Bars, 50 μm (A–H). (This figure is available in colour at JXB online.)

The *elp2* mutant has a reduced auxin content in root tip

Auxin gradients (Vanneste and Friml, 2009) are central to the robust development of the primary root in *Arabidopsis*, and the auxin gradient in the root tip could be instructive for the patterning of root distal stem cell (DSC) niches (Tian *et al.*, 2013, 2014). To substantiate if the root defective phenotypes in *elp2* are resulting from the changed auxin signalling in root

tips, *DR5rev*:*GFP* and *DR5*:*GUS* synthetic auxin response reporters (Friml *et al.*, 2003) were used to assay auxin signalling. The signal from both reporters was markedly lower in the mutant than in the WT root tip (Fig. 6A–D). The GUS enzyme activity assay using the MUG as the substrate further confirmed this difference (data not shown). Furthermore, we measured the free IAA content in roots of the *elp2* mutant. Consistently, the *elp2* mutant has reduced IAA content in roots compared to the wild-type control (Fig. 6E).

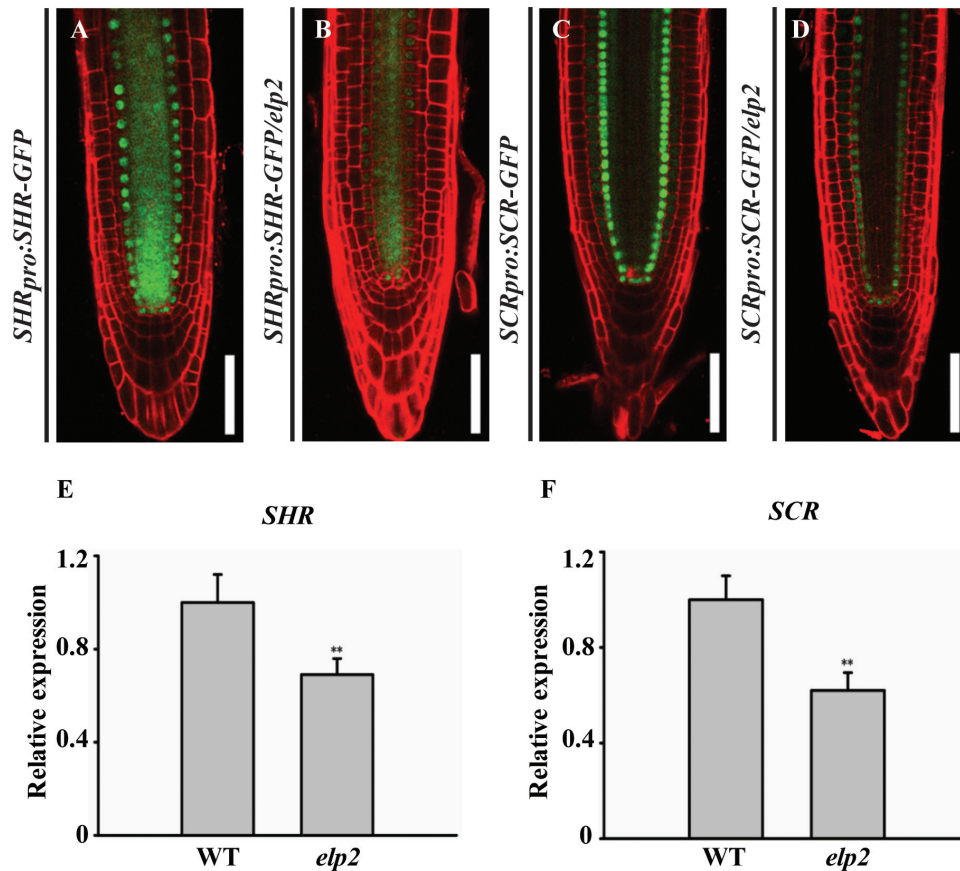


Fig. 4. *SHR* and *SCR* expression is reduced in the *elp2* mutant. Expression of the transgenes (A, B) *SHR pro:SHR-GFP*, (C, D) *SCR pro:SCR-GFP*. qRT-PCR assay of the transcription of (E) *SHR* and (F) *SCR*. The data represent mean values with their associated SD ($n=3$); **, $P<0.001$. Bars, 50 μm (A–D). (This figure is available in colour at JXB online.)

Auxin polar transport was affected in elp2

To address if the reduced auxin signalling in root tips of *elp2* was a result of the affected polar auxin transport, we examined the polar localization of auxin efflux carriers such as PIN1 and PIN2 (Petrasek et al., 2006), which mediate auxin distribution in plants, including to the roots (Blilou et al., 2005; Wisniewska et al., 2006). Basal localized PIN1 in the stele and basal localized PIN2 in the cortex contribute to auxin transportation from shoot to root, thus contributing to maximum auxin formation in root tips and regulating root growth (Galweiler et al., 1998; Friml et al., 2003; Blilou et al., 2005; Wisniewska et al., 2006). However, in *elp2*, basal localization of PIN1 is less polar, and the increased lateral localization of PIN1 was observed from both our immunolocalization examinations with the anti-PIN1 antibody and confocal examinations with the *PIN1-GFP* line (Fig. 7A–D). Though apical PIN2 in the epidermis displays WT polarity in *elp2* (Fig. 7E–H), both the protein expression levels of PIN1 and PIN2 were reduced in *elp2* (Fig. 7C, D, G, H).

Previous studies have already demonstrated that PP2A and PINOID partially colocalize with PINs and act antagonistically on the phosphorylation state of PINs hydrophilic loop (Benjamins et al., 2001; Michniewicz et al., 2007; Huang et al., 2010). 35S:*PID* seedlings have basal to apical localization of PIN1 (Michniewicz et al., 2007). Thus, we examined

the *PINOID* expression in the *elp2* mutant. We found the *elp2* mutant to have a consistently higher expression level of *PINOID* compared with the WT control (Fig. 7I).

ELP2 affects the histone acetylation levels of several key transcription factor genes

The histone acetyltransferase of ELP3 has been confirmed both in yeast and plants (Winkler et al., 2002; Nelissen et al., 2010). To address whether the reduced expression level of several key transcription factors encoding genes such as *PLT1*, *PLT2*, *SCR* and *SHR* in *elp2* may be associated with the reduced acetylation levels, we performed CHIP-PCR using an antibody specific for histone H3 acetylated at Lys-9 and -14 (H3K9/14ac). CHIP-PCR was performed to verify whether the reduced expression of *PLT1*, *PLT2*, *SCR* and *SHR* in the mutant was correlated with the altered acetylation level. The assay based on primers targeting the coding region and the 5'-UTR of *PLT1* and *PLT2* showed that acetylation in this part of the gene was markedly reduced in the mutant (Fig. 8), while the acetylation level of the internal reference gene *ACTIN2* was not changed (Supplementary Fig. S5A). A similar result was obtained with respect to the *SHR* and *SCR* coding regions which show reduced acetylation, but there was no difference between the WT and the mutant within promoter regions of both genes (Fig. 8). In addition, we also found a

reduced acetylation level in 3' coding region of *PIN1*, consistent with the reduced expression level of *PIN1* (Supplementary Fig. S5B).

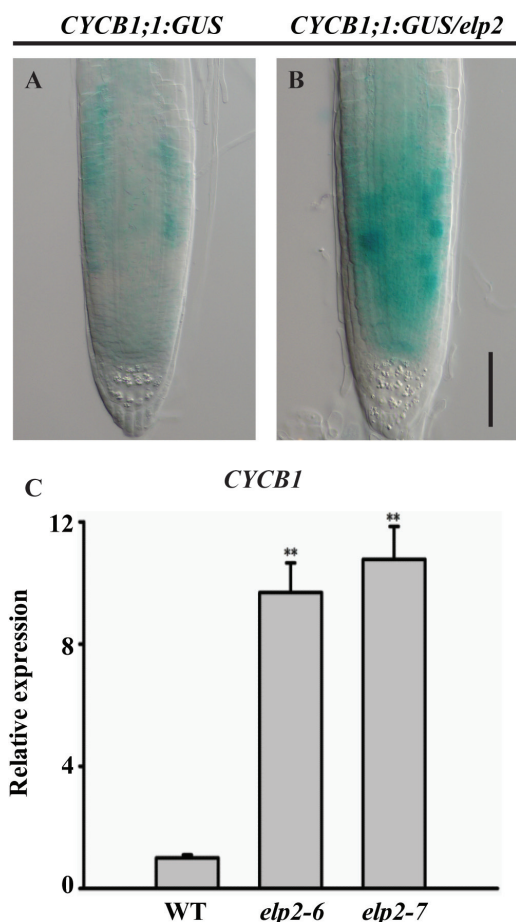


Fig. 5. *CYCB1* expression is increased in the *elp2* mutant. (A, B) Expression of the *CYCB1;1:GUS* transgene, (C) transcription of *CYCB1* assayed by qRT-PCR. The data represent mean values with their associated SD, ($n=3$); **, $P<0.001$. Bars, 50 μm (A, B). (This figure is available in colour at JXB online.)

ELP2 is required for the DNA methylation of *CYCB1* but not of *PID*, *SHR* or *SCR*

ELP2 has recently been reported to be involved in somatic DNA demethylation/methylation, thus regulating pathogen-induced transcriptome reprogramming and plant immune responses (Wang *et al.*, 2013). To address the reduced expression levels of transcription factors such as *SCR* and *SHR*, the increased expression of *PID*, and whether the increased expression of the cell cycle gene *CYCB1* in *elp2* are associated with the altered methylation levels, DNA methylation levels in *CYCB1*, *PID*, *SHR* and *SCR* were estimated by bisulfite sequencing. The level of methylation throughout both the promoter and coding regions of *PID*, *SHR* and *SCR* was low (Supplementary Figs S6, S7), indicating that these genes are not under the control of DNA demethylation/methylation. In the *CYCB1* promoter, five cytosines showed a reduced frequency of methylation in the *elp2* mutant compared to the WT. The mutant sequence was less methylated at the 3' end of its coding region (Fig. 9). The observed reduced level of methylation in this gene was consistent with its up-regulation in the mutant.

Discussion

ELP2 is one of a six-subunit (*ELP1* to 6) protein complex first isolated from yeast (Wittschieben *et al.*, 1999), and later termed 'elongator' on the basis that it was co-purified with the hyper-phosphorylated form of RNA polymerase II. The complex has been shown to support transcription via the regulation of DNA methylation, histone acetylation or tRNA modification (Winkler *et al.*, 2002; Chen *et al.*, 2009; Wang *et al.*, 2013). In plants, its activity has been associated with growth and development, pathogen defence, and responses to abiotic stress. *elp1*, *elp3* and *elp4* have been reported to regulate root growth (Nelissen *et al.*, 2005), although the underlying mechanism of this control has not yet been well

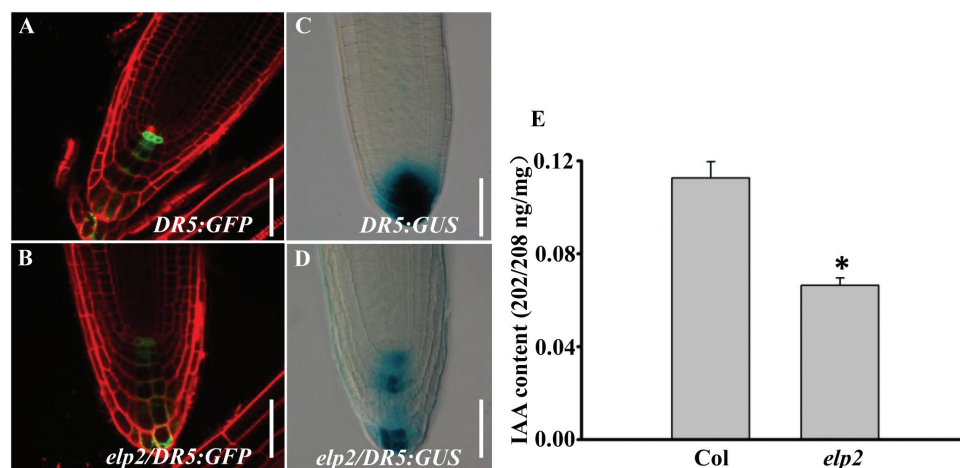


Fig. 6. The *elp2* mutant exhibits reduced auxin contents in roots. (A, B) The mutant shows a reduced level of *DR5rev:GFP* expression in the root than the WT. (C, D) The mutant shows a reduced level of *DR5:GUS* expression in the root than the WT. (E) IAA content measurement of roots on 14-day-old seedlings of col and *elp2*. The data represent mean values of three independent biological repeats with their associated SD ($n=3$), $P<0.05$. Bars, 50 μm (A–D). (This figure is available in colour at JXB online.)

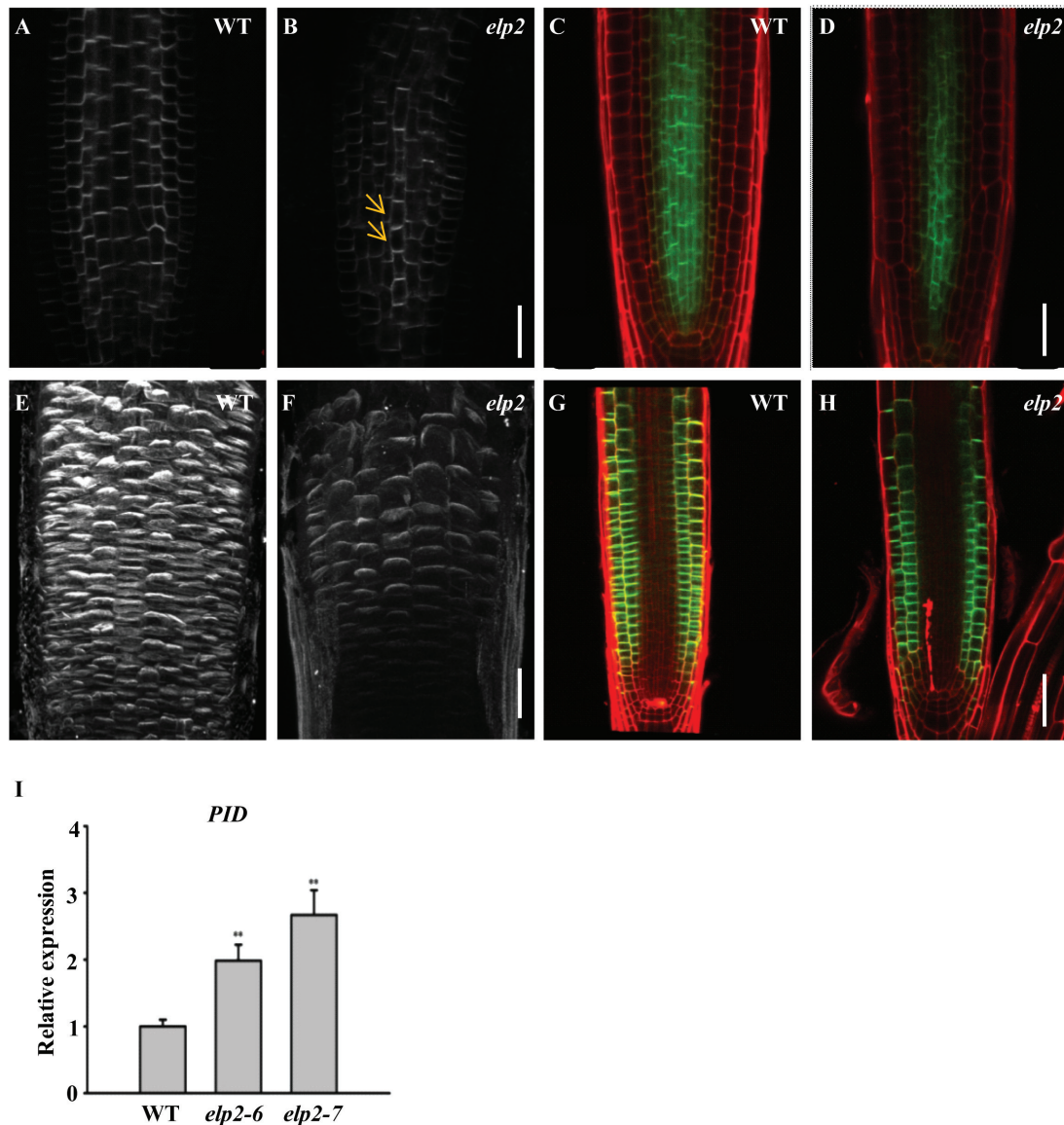


Fig. 7. PIN1 and PIN2 localization and expression in the *elp2* mutant. (A, B) PIN1 immunolocalization in five-day-old roots. (C, D) Expression and polarity of PIN1:PIN1-GFP in the WT and mutant root. (E, F) PIN2 immunolocalization in five-day old roots. (G, H) Expression and polarity of PIN2:PIN2-GFP in the WT and mutant root. (I) *PID* transcription assayed by qRT-PCR. The data represent mean values with their associated SD ($n=3$); **, $P<0.001$. Bars, 50 μm (A–H). (This figure is available in colour at JXB online.)

elucidated. Here, we demonstrated that *ELP2* also acts as a regulator of root growth, via its effect on the maintenance of the root stem cell niche. The basis of the regulation was the epigenetic modification of the transcription factors *SCR*, *SHR*, *PLT1* and *PLT2*, and the G2/M transition activator *CYCBI*.

The role of *ELP2* in root development

A systematic contrast in root growth and development between WT and the *elp2* loss-of-function mutant showed that the absence of *ELP2* caused root foreshortening as a result of a reduction in cell size in the EZ and in cell number in the MZ. In addition, the mutant was also defective with respect to root stem cell niche maintenance, exhibiting a much increased rate of cell division in the QC and an accelerated

differentiation of the root distal stem cells. The mutants *scr*, *shr* and *plt1plt2* were not only compromised with respect to their root growth, but also experienced increased cell division in the QC and accelerated differentiation of their root distal stem cells (Helariutta *et al.*, 2000; Sabatini *et al.*, 2003; Aida *et al.*, 2004; Galinha *et al.*, 2007). A clear hypothesis therefore was that the loss of *ELP* interfered with the functioning of *SCR*, *SHR*, *PLT1* and *PLT2*. The knockdown of *WOX5*, the product of which is specifically deposited in the QC (Sarkar *et al.*, 2007; Forzani *et al.*, 2014), may also have contributed to the defective root stem cell niche maintenance shown by the *elp2* mutant. It has been established that an optimized level of auxin signalling in the QC is required to ensure root stem cell identity. QC-centered auxin gradients are formed by polar auxin transport and local auxin synthesis (Grieneisen *et al.*, 2007; Tian *et al.*, 2013). Disturbing the optimal level

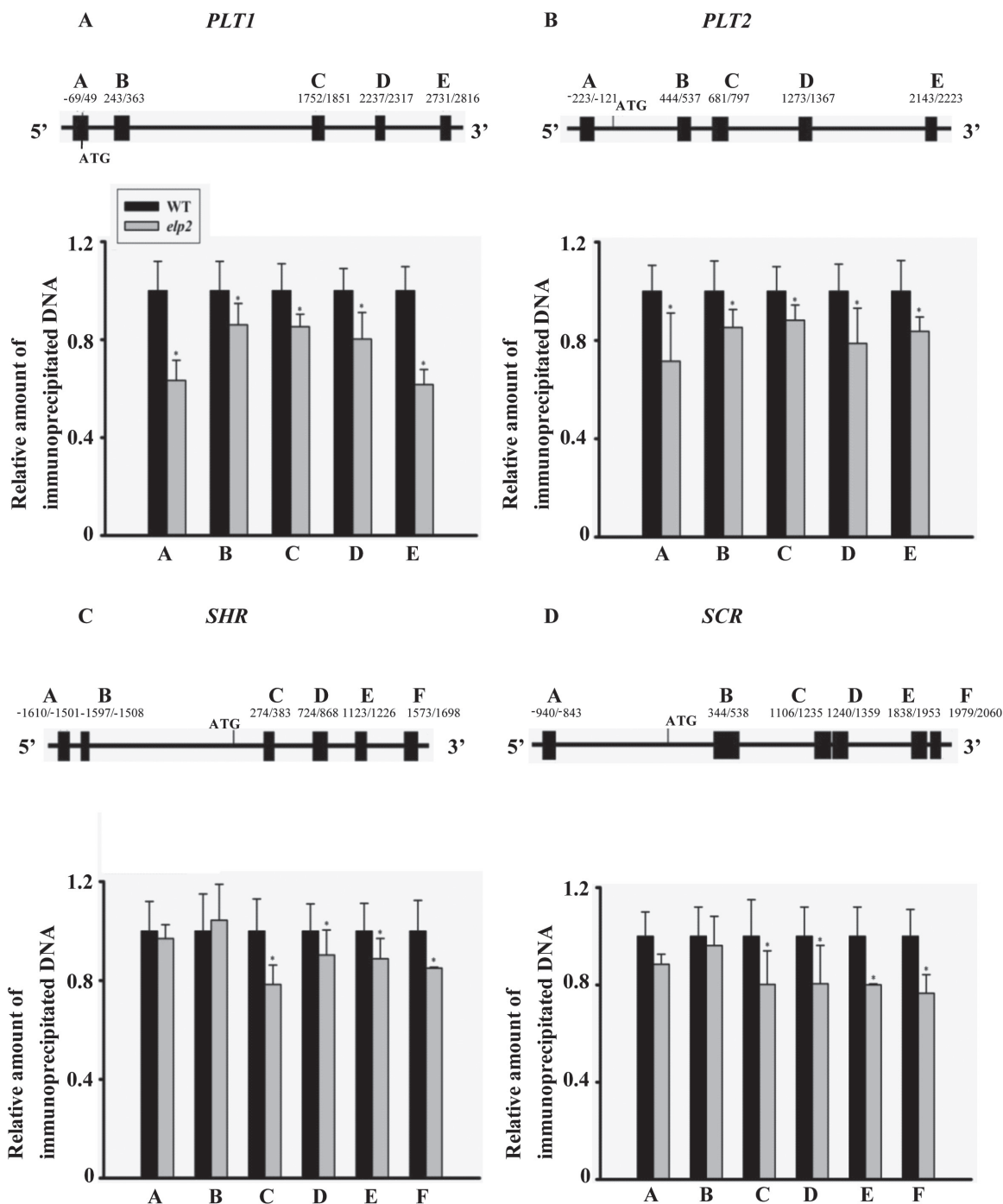


Fig. 8. Histone H3 acetylation levels in (A) *PLT1*, (B) *PLT2*, (C) *SHR* and (D) *SCR*. The placement of the primers is indicated. The relative amount of immunoprecipitated chromatin fragments in the *elp2* mutant, as determined by qRT-PCR, was compared to that produced in the WT. The data represent mean values with their associated SD ($n=3$); *, $P<0.05$.

favours accelerated differentiation of the root distal stem cells (Tian *et al.*, 2013, 2014), so a reduction in auxin supply to the mutants' root tips may also have made a contribution to its root phenotype.

ELP2 epigenetically affects the transcription of genes involved in root meristem maintenance

The elongator complex acts to acetylate both core histones and nucleosomal substrates (Winkler *et al.*, 2002).

In *A. thaliana elp3* mutant, histone H3 lysine 14 acetylation level is reduced in the coding region of both *SHORT HYPOCOTYL 2* (auxin repressor) and *LAX2* (auxin influx carrier), resulting in a reduction in their expression and hence the mutant's phenotype (Nelissen *et al.*, 2010). The loss of *ELP2* similarly reduces acetylation level in the coding region of the GRAS family transcription factors *SCR* and *SHR*, and that of the AP2 transcription factors *PLT1* and *PLT2*, thereby down-regulating them all. The result underlines the requirement that each of the elongator complex components

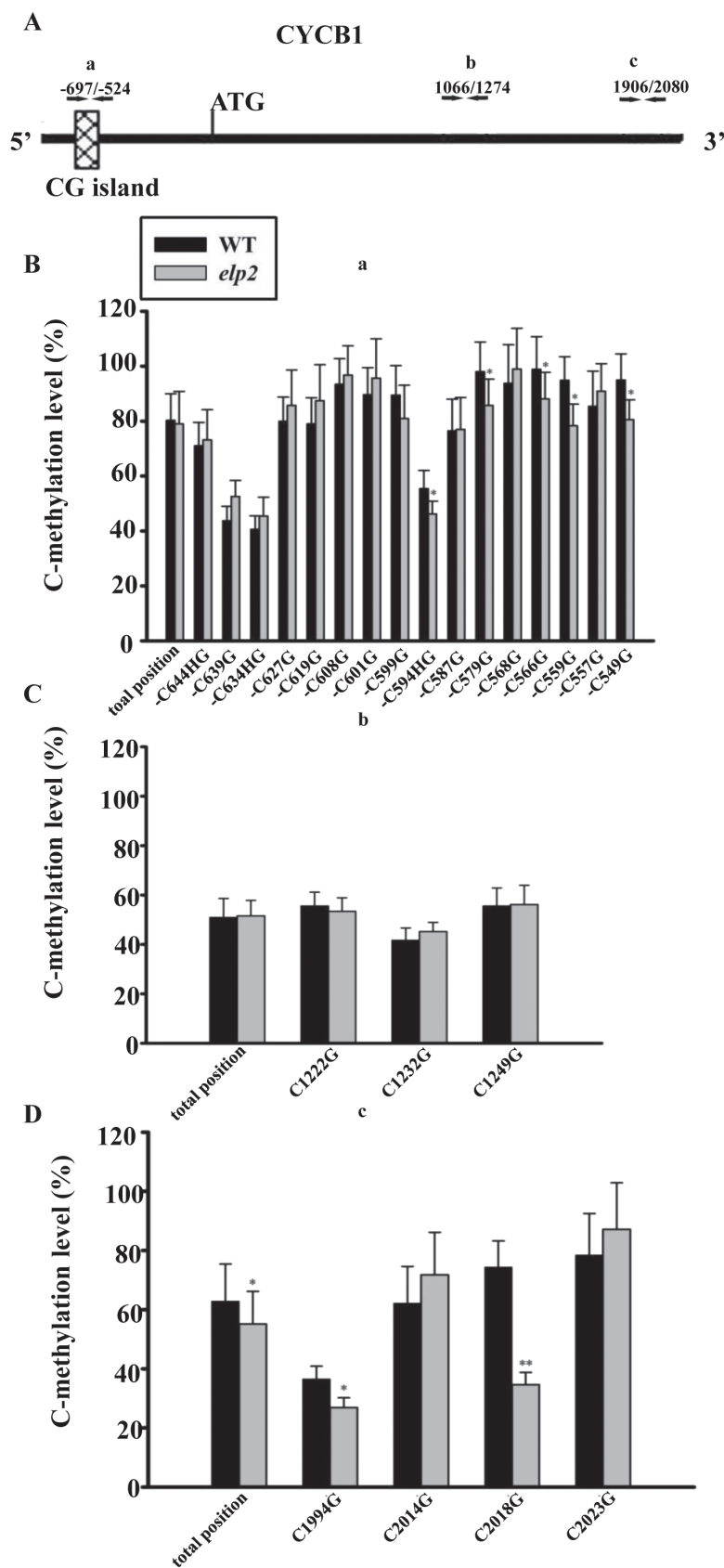


Fig. 9. DNA methylation level is altered in the *elp2* mutant. (A) Placement of the primers is indicated. The rectangular box represents a CG island. (B–D) The methylation level of amplified fragments a (B), b (C) and c (D). The DNA was extracted from three biological replicates of both WT and *elp2*. Three replicates of 60 clones derived from each of WT and *elp2* were bisulfite-sequenced to assess their methylation level. The data represent mean values with their associated SD ($n=3$); *, $P<0.05$, **, $P<0.001$.

be present if complex assembly, integrity and enzymatic activity are to proceed normally (Glatt and Muller, 2013). DNA methylation is a central process regulating many of the genes involved in growth and the response to the plant's environment (Chinnusamy and Zhu, 2009; He *et al.*, 2011; Li *et al.*, 2012; Wang *et al.*, 2013). *ELP2* has been recently shown to contribute to DNA methylation (Wang *et al.*, 2013). Consistent with the generally observed negative correlation between DNA methylation and gene expression, the up-regulation of *CYCB1* in the *elp2* mutant may reflect its reduced level of methylation within both the promoter and/or coding region.

ELP2 affects auxin signal in root tip

An optimal auxin maximum is required to maintain root stem cell niche identity and root growth (Grieneisen *et al.*, 2007; Tian *et al.*, 2013, 2014). The *elp2* mutant has reduced IAA content in roots, indicating that the *ELP2* interferes with the auxin homeostasis regulation. The basal auxin efflux carrier PIN1 drives the flow of auxin from the stele towards the root tip (Galweiler *et al.*, 1998; Blilou *et al.*, 2005; Wisniewska *et al.*, 2006; Grieneisen *et al.*, 2007), while PIN2 controls its flow from the cortex (Blilou *et al.*, 2005; Wisniewska *et al.*, 2006). In the *elp2* mutant, the less polarized PIN1 and decreased levels of both PIN1 and PIN2 reduced the supply of auxin to root tip. Therefore, the *elp2* mutant has reduced auxin signal in the root, which could break the stem cell niche maintenance.

Supplementary data

Supplementary data are available at *JXB* online.

Supplementary Figure S1. Agarose gel analysis of TAIL-PCR products amplified from WT and *drs1 (elp2)* genomic DNA

Supplementary Figure S2. The structure of *elp2*.

Supplementary Figure S3. Micrographs of the root stem cell niche in (A) WT, (B) *elp2-6*, (C), *elp2-7*, (D) *elp1*, (E) *elp4* and (F) *elp6*.

Supplementary Figure S4. *elp* mutants have short primary roots.

Supplementary Figure S5. Histone H3 acetylation levels in (A) *ACTIN2*, (B) *PIN1*.

Supplementary Figure S6. Levels of methylation in (A) *SHR* and (B) *SCR*.

Supplementary Figure S7. DNA methylation level assay of the *PINOID*.

Supplementary Table S1. Summary of primers used in this study.

Acknowledgements

ZD is supported by grants from the Ministry of Science and Technology of China (2015CB942901) and the National Natural Science Foundation of China (Projects 31470371, 31270327 and 31222005). HT is supported by the National Natural Science Foundation of Shandong (ZR2013CQ042). The authors acknowledge B. Scheres, T. Laux, Z.-H. Gong, C.-Y. Li, Z.-L. Mou

and P Benfey for published materials. We also like to give our special thanks to Prof. Chuanyou Li for the helpful discussions and suggestions in this study.

References

- Aida M, Beis D, Heidstra R, Willemsen V, Blilou I, Galinha C, Nussaume L, Noh YS, Amasino R, Scheres B. 2004. The PLETHORA genes mediate patterning of the *Arabidopsis* root stem cell niche. *Cell* **119**, 109–120.
- Benjamins R, Quint A, Weijers D, Hooykaas P, Offringa R. 2001. The PINOID protein kinase regulates organ development in *Arabidopsis* by enhancing polar auxin transport. *Development* **128**, 4057–4067.
- Benjamins R, Scheres B. 2008. Auxin: the looping star in plant development. *Annual Review of Plant Biology* **59**, 443–465.
- Benkova E, Michniewicz M, Sauer M, Teichmann T, Seifertova D, Jurgens G, Friml J. 2003. Local, efflux-dependent auxin gradients as a common module for plant organ formation. *Cell* **115**, 591–602.
- Blilou I, Xu J, Wildwater M, Willemsen V, Paponov I, Friml J, Heidstra R, Aida M, Palme K, Scheres B. 2005. The PIN auxin efflux facilitator network controls growth and patterning in *Arabidopsis* roots. *Nature* **433**, 39–44.
- Chen C, Huang B, Eliasson M, Ryden P, Bystrom AS. 2011. Elongator complex influences telomeric gene silencing and DNA damage response by its role in wobble uridine tRNA modification. *PLoS Genetics* **7**, e1002258.
- Chen C, Tuck S, Bystrom AS. 2009. Defects in tRNA modification associated with neurological and developmental dysfunctions in *Caenorhabditis elegans* elongator mutants. *PLoS Genetics* **5**, e1000561.
- Chinnusamy V, Zhu JK. 2009. Epigenetic regulation of stress responses in plants. *Current Opinion in Plant Biology* **12**, 133–139.
- Colon-Carmona A, You R, Haimovitch-Gal T, Doerner P. 1999. Technical advance: spatio-temporal analysis of mitotic activity with a labile cyclin-GUS fusion protein. *The Plant Journal* **20**, 503–538.
- Creppe C, Malinetskaya L, Volvert ML, *et al.* 2009. Elongator controls the migration and differentiation of cortical neurons through acetylation of alpha-tubulin. *Cell* **136**, 551–564.
- Dai M, Zhang C, Kania U, *et al.* 2012. A PP6-type phosphatase holoenzyme directly regulates PIN phosphorylation and auxin efflux in *Arabidopsis*. *The Plant Cell* **24**, 2497–514.
- Defraia CT, Wang Y, Yao J, Mou Z. 2013. Elongator subunit 3 positively regulates plant immunity through its histone acetyltransferase and radical S-adenosylmethionine domains. *BMC Plant Biology* **13**, 102.
- DeFraia CT, Zhang X, Mou Z. 2010. Elongator subunit 2 is an accelerator of immune responses in *Arabidopsis thaliana*. *The Plant Journal* **64**, 511–523.
- Dello Iorio R, Linhares FS, Scacchi E, Casamitjana-Martinez E, Heidstra R, Costantino P, Sabatini S. 2007. Cytokinins determine *Arabidopsis* root-meristem size by controlling cell differentiation. *Current Biology* **17**, 678–682.
- Dello Iorio R, Nakamura K, Moubayidin L, Perilli S, Taniguchi M, Morita MT, Aoyama T, Costantino P, Sabatini S. 2008. A genetic framework for the control of cell division and differentiation in the root meristem. *Science* **322**, 1380–1384.
- Di Laurenzio L, Wysocka-Diller J, Malamy JE, Pysh L, Helariutta Y, Freshour G, Hahn M G, Feldmann KA, Benfey PN. 1996. The SCARECROW gene regulates an asymmetric cell division that is essential for generating the radial organization of the *Arabidopsis* root. *Cell* **86**, 423–433.
- Ding Z, Friml J. 2010. Auxin regulates distal stem cell differentiation in *Arabidopsis* roots. *Proceedings of the National Academy of Sciences, USA* **107**, 12046–12051.
- Dolan L, Janmaat K, Willemsen V, Linstead P, Poethig S, Roberts K, Scheres B. 1993. Cellular organisation of the *Arabidopsis thaliana* root. *Development* **119**, 71–84.
- Forzani C, Aichinger E, Sornay E, Willemsen V, Laux T, Dewitte W, Murray JA. 2014. WOX5 suppresses CYCLIN D activity to establish quiescence at the center of the root stem cell niche. *Current Biology* **24**, 1939–1944.
- Friml J, Vieten A, Sauer M, Weijers D, Schwarz H, Hamann T, Offringa R, Jurgens G. 2003. Efflux-dependent auxin gradients establish the apical-basal axis of *Arabidopsis*. *Nature* **426**, 147–153.

- Galinha C, Hofhuis H, Luijten M, Willemsen V, Blilou I, Heidstra R, Scheres B.** 2007. PLETHORA proteins as dose-dependent master regulators of *Arabidopsis* root development. *Nature* **449**, 1053–1057.
- Galweiler, L, Guan, C, Muller, A, Wisman, E, Mendgen, K, Yephremov, A, Palme, K** 1998. Regulation of polar auxin transport by AtPIN1 in *Arabidopsis* vascular tissue. *Science* **282**, 2226–2230.
- Glatt S, Muller CW.** 2013. Structural insights into elongator function. *Current Opinion in Structural Biology* **23**, 235–242.
- Grieneisen VA, Xu J, Maree AF, Hogeweg P, Scheres B.** 2007. Auxin transport is sufficient to generate a maximum and gradient guiding root growth. *Nature* **449**, 1008–1013.
- He XJ, Chen T, Zhu JK.** 2011. Regulation and function of DNA methylation in plants and animals. *Cell Research* **21**, 442–465.
- Helariutta Y, Fukaki H, Wysocka-Diller J, Nakajima K, Jung J, Sena G, Hauser MT, Benfey PN.** 2000. The SHORT-ROOT gene controls radial patterning of the *Arabidopsis* root through radial signaling. *Cell* **101**, 555–567.
- Huang F, Zago MK, Abas L, van Marion A, Galvan-Ampudia CS, Offringa R.** 2010. Phosphorylation of conserved PIN motifs directs *Arabidopsis* PIN1 polarity and auxin transport. *The Plant Cell* **22**, 1129–1142.
- Kim JH, Lane WS, Reinberg D.** 2002. Human elongator facilitates RNA polymerase II transcription through chromatin. *Proceedings of the National Academy of Sciences, USA* **99**, 1241–1246.
- Kornet N, Scheres B.** 2009. Members of the GCN5 histone acetyltransferase complex regulate PLETHORA-mediated root stem cell niche maintenance and transit amplifying cell proliferation in *Arabidopsis*. *The Plant Cell* **21**, 1070–1079.
- Li X, Qian W, Zhao Y, Wang C, Shen J, Zhu JK, Gong Z.** 2012. Antisilencing role of the RNA-directed DNA methylation pathway and a histone acetyltransferase in *Arabidopsis*. *Proceedings of the National Academy of Sciences, USA* **109**, 11425–11430.
- Michniewicz M, Zago MK, Abas L, et al.** 2007. Antagonistic regulation of PIN phosphorylation by PP2A and PINOID directs auxin flux. *Cell* **130**, 1044–1056.
- Mosher RA, Durrant WE, Wang D, Song J, Dong X.** 2006. A comprehensive structure-function analysis of *Arabidopsis* SNI1 defines essential regions and transcriptional repressor activity. *The Plant Cell* **18**, 1750–1765.
- Nakajima K, Sena G, Nawy T, Benfey PN.** 2001. Intercellular movement of the putative transcription factor SHR in root patterning. *Nature* **413**, 307–311.
- Nelissen H, De Groeve S, Fleury D, et al.** 2010. Plant Elongator regulates auxin-related genes during RNA polymerase II transcription elongation. *Proceedings of the National Academy of Sciences, USA* **107**, 1678–1683.
- Nelissen H, Fleury D, Bruno L, Robles P, De Veylder L, Traas J, Micol JL, Van Montagu M, Inze D, Van Lijsebettens M.** 2005. The elongata mutants identify a functional elongator complex in plants with a role in cell proliferation during organ growth. *Proceedings of the National Academy of Sciences, USA* **102**, 7754–7759.
- Petrasek J, Mravec J, Bouchard R, et al.** 2006. PIN proteins perform a rate-limiting function in cellular auxin efflux. *Science* **312**, 914–8.
- Rahl PB, Chen CZ, Collins RN.** 2005. Elp1p, the yeast homolog of the FD disease syndrome protein, negatively regulates exocytosis independently of transcriptional elongation. *Molecular Cell* **17**, 841–53.
- Ruzicka K, Simaskova M, Duclercq J, Petrasek J, Zazimalova E, Simon S, Friml J, Van Montagu MC, Benkova E.** 2009. Cytokinin regulates root meristem activity via modulation of the polar auxin transport. *Proceedings of the National Academy of Sciences, USA* **106**, 4284–4289.
- Sabatini S, Heidstra R, Wildwater M, Scheres B.** 2003. SCARECROW is involved in positioning the stem cell niche in the *Arabidopsis* root meristem. *Genes and Development* **17**, 354–358.
- Sarkar AK, Luijten M, Miyashima S, Lenhard M, Hashimoto T, Nakajima K, Scheres B, Heidstra R, Laux T.** 2007. Conserved factors regulate signalling in *Arabidopsis* thaliana shoot and root stem cell organizers. *Nature* **446**, 811–814.
- Tian H, Niu T, Yu Q, Quan T, Ding Z.** 2013. Auxin gradient is crucial for the maintenance of root distal stem cell identity in *Arabidopsis*. *Plant Signaling & Behavior* **8**, e26429.
- Tian H, Wabnik K, Niu T, et al.** 2014. WOX5-IAA17 feedback circuit-mediated cellular auxin response is crucial for the patterning of root stem cell niches in *Arabidopsis*. *Molecular Plant* **7**, 277–289.
- Ulmason T, Murfett J, Hagen G, Guilfoyle TJ.** 1997. Aux/IAA proteins repress expression of reporter genes containing natural and highly active synthetic auxin response elements. *The Plant Cell* **9**, 1963–1971.
- Vanneste S, Friml J.** 2009. Auxin: a trigger for change in plant development. *Cell* **136**, 1005–1016.
- Vanstraelen M, Balaban M, Da Ines O, Cultrone A, Lammens T, Boudolf V, Brown SC, De Veylder L, Mergaert P, Kondorosi E.** 2009. APC/C-CCS52A complexes control meristem maintenance in the *Arabidopsis* root. *Proceedings of the National Academy of Sciences, USA* **106**, 11806–11811.
- Vernoux T, Benfey PN.** 2005. Signals that regulate stem cell activity during plant development. *Current Opinion in Genetics & Development* **15**, 388–394.
- Versees W, De Groeve S, Van Lijsebettens M.** 2010. Elongator, a conserved multitasking complex? *Molecular Microbiology* **76**, 1065–1069.
- Wang Y, An C, Zhang, X, Yao J, Zhang Y, Sun Y, Yu F, Amador D M, Mou Z.** 2013. The *Arabidopsis* elongator complex subunit2 epigenetically regulates plant immune responses. *The Plant Cell* **25**, 762–776.
- Weingartner M, Criqui MC, Meszaros T, Binarova P, Schmit AC, Helfer A, Derevier A, Erhardt M, Bogre L, Genschik P.** 2004. Expression of a nondegradable cyclin B1 affects plant development and leads to endomitosis by inhibiting the formation of a phragmoplast. *The Plant Cell* **16**, 643–657.
- Winkler GS, Kristjuhan A, Erdjument-Bromage H, Tempst P, Svejstrup JQ.** 2002. Elongator is a histone H3 and H4 acetyltransferase important for normal histone acetylation levels in vivo. *Proceedings of the National Academy of Sciences, USA* **99**, 3517–22.
- Wisniewska J, Xu J, Seifertova D, Brewer PB, Ruzicka K, Blilou I, Rouquie D, Benkova E, Scheres B, Friml J.** 2006. Polar PIN localization directs auxin flow in plants. *Science* **312**, 883.
- Wittschieben BO, Otero G, de Bizemont T, Fellows J, Erdjument-Bromage H, Ohba R, Li Y, Allis CD, Tempst P, Svejstrup JQ.** 1999. A novel histone acetyltransferase is an integral subunit of elongating RNA polymerase II holoenzyme. *Molecular Cell* **4**, 123–128.
- Xu D, Huang W, Li Y, Wang H, Huang H, Cui X.** 2011. Elongator complex is critical for cell cycle progression and leaf patterning in *Arabidopsis*. *The Plant Journal* **69**, 792–808.
- Zhou X, Hua D, Chen Z, Zhou Z, Gong Z.** 2009. Elongator mediates ABA responses, oxidative stress resistance and anthocyanin biosynthesis in *Arabidopsis*. *The Plant Journal* **60**, 79–90.